^{123}I-Hippuran Renal Scintigraphy with Evaluation of Single-Kidney Clearance for Predicting Renal Scarring After Acute Urinary Tract Infection: Comparison with ^{99m}Tc-DMSA Scanning

Alessio Imperiale, MD[1]; Catia Olianti, MD[1]; Stelvio Sestini, MD[1]; Marco Materassi, MD[2]; Seracini Daniela, MD[2]; Rita Ienuso, MD[3]; and Giuseppe La Cava, MD[1]

[1]Nuclear Medicine Unit, Department of Clinical Pathophysiology, University of Florence, Florence, Italy; [2]Department of Pediatrics, University of Florence, Florence, Italy; and [3]Department of Radiology, "Anna Meyer" Pediatric Hospital, Florence, Italy

The value of ^{123}I-hippuran (OIH) renal sequential scintigraphy (RSS) in predicting the evolution of defects detected by ^{99m}Tc-dimercaptosuccinic acid (DMSA) scanning during a first episode of acute pyelonephritis (APN) was assessed. **Methods:** Fifty-eight children with APN underwent ^{99m}Tc-DMSA planar scanning and ^{123}I-OIH RSS during acute infection and at least 5 mo later. Renal lesions found by ^{99m}Tc-DMSA scanning were classified according to the following ^{99m}Tc-DMSA grading system: 0 = normal, 1 = 1 lesion, 2 = 2 lesions, and 3 = diffuse damage with renal parenchymal subversion. Renal scarring was diagnosed whenever a renal cortical defect detected at the first ^{99m}Tc-DMSA examination persisted on the follow-up ^{99m}Tc-DMSA examination. Single-kidney clearance rate (*Cl*) was evaluated by a method that was previously validated at our institution and is based on time–activity curves measured on the heart and kidney areas by the region-of-interest technique. **Results:** ^{99m}Tc-DMSA scanning showed renal damage in 76 kidneys and had negative findings for the remaining 40 kidneys (2 patients had bilaterally negative findings). ^{99m}Tc-DMSA scanning determined 40 kidneys to be grade 0, 49 to be grade 1, 21 to be grade 2, and 6 to be grade 3. For ^{99m}Tc-DMSA grades of 0–3, the corresponding *Cl* mean values (in mL/min/1.73 m^2 of body surface area [BSA]) were 292 ± 33, 237 ± 39, 210 ± 54, and 140 ± 53, respectively. The Spearman regression coefficient (*R*) demonstrated a significant correlation between ^{99m}Tc-DMSA grade and *Cl* ($R = 0.69$, $P < 0.0001$). Thirty-six of the lesions detected by staging ^{99m}Tc-DMSA were shown to have recovered on follow-up renal scans, whereas 40 developed scars. A significant difference in *Cl* was found between the 2 groups ($P < 0.0002$). The *Cl* cutoff value was determined by univariate discriminant analysis; a *Cl* value of 232 mL/min/1.73 m^2 of BSA discriminated best between scarred and nonscarred kidneys, with a specificity, sensitivity, positive predictive value, negative predictive value, and overall accuracy of 95%, 95%, 90%, 97%, and 95%, respectively. **Conclusion:** *Cl* evaluation, in the course of acute urinary tract infection, is highly valuable in predicting the fibrotic evolution of renal damage detected on acute ^{99m}Tc-DMSA scanning. Also, our data show close agreement between *Cl* and the grade determined by staging ^{99m}Tc-DMSA.

Key Words: urinary tract infection; ^{99m}Tc-DMSA; pediatric acute pyelonephritis; ^{123}I-hippuran

J Nucl Med 2003; 44:1755–1760

Renal parenchymal acute infection (acute pyelonephritis, or APN), one of the most common pediatric diseases, may be associated with permanent functional renal damage followed by important sequelae such as hypertension, proteinuria, and areas of renal fibrosis (scarring) (*1–3*). Hence, accurate, well-timed, and correct diagnosis is a major challenge for the therapeutic management of children with a real risk of kidney scarring.

^{99m}Tc-Dimercaptosuccinic acid (DMSA) static planar imaging is able to identify parenchymal injury as a focal area of radiopharmaceutical fixation defect. Thus, this method is already considered the gold standard imaging technique for the diagnosis of APN, especially for children without previous renal abnormalities. It has largely been proven that the sensitivity of ^{99m}Tc-DMSA in detecting renal cortical abnormalities is higher than that of either intravenous pyelography or sonography (*4,5*). ^{99m}Tc-DMSA scanning provides clinically useful indexes of absolute renal function and relative renal function (differential renal function, or DRF), particularly effective in follow-up (*6–8*).

Parenchymal scarring most likely occurs in younger patients, in children with congenital urinary tract abnormalities (i.e., vesicoureteral reflux), and in patients for whom ^{99m}Tc-DMSA scanning shows multifocal lesions in the acute phase (*3*). Despite that, not all defects found on ^{99m}Tc-DMSA scanning during the APN episode develop into permanent lesions.

Received Feb. 20, 2003; revision accepted Jun. 13, 2003.

For correspondence or reprints contact: Giuseppe La Cava, MD, Nuclear Medicine Unit, Department of Clinical Pathophysiology, University of Florence, Viale Morgagni 85, 50134 Florence, Italy.

E-mail: g.lacava@dfc.unifi.it

However, no definitive criteria have been established to predict whether an acute lesion will evolve into permanent renal damage. Some recent reports proposed the DRF index as a quantitative parameter to predict the evolution of renal scarring, but that proposal has not yet won common agreement (*6–7*).

The aim of this study was to evaluate the relationship between renal abnormalities found on ^{99m}Tc-DMSA scans and single-kidney clearance rate (*Cl*) estimated by ^{123}I-hippuran (OIH) renal sequential scintigraphy (RSS) during the acute phase of urinary tract infection (UTI). Particularly, the purpose was to estimate the possible role of RSS as a predictor of the further evolution of defects detected by ^{99m}Tc-DMSA scanning.

MATERIALS AND METHODS

Patient Population

Among children admitted to our Pediatric Unit during a 2-y period, 58 (21 boys, 37 girls; age range, 0.5–54 mo; mean age, 7.2 ± 12.4 mo) with signs and symptoms suggestive of APN (*3*) were selected for this study. The inclusion criteria were the following: age less than 10 y, no history of previous UTI, no hypodysplasia pattern on either prenatal or routine sonography, no urinary tract obstruction causing secondary reflux, and no recurrent infection between the initial (during the APN phase) and subsequent ^{99m}Tc-DMSA examinations.

With a renal unit defined as 1 kidney and its ureter, 116 renal units were examined.

The diagnosis of APN was based on both clinical examination (unexplained fever, irritability, vomiting, diarrhea, and failure to thrive) and laboratory examinations (quantitative C-reactive protein, sedimentation rate, white blood cell count, and catheterized urine culture) (*3*). The urine culture was considered positive if the number of colonies of a single organism (CFU) was $\geq 10^5$/mL.

For confirmation of the clinical and laboratory diagnosis of APN, all children underwent renal and pelvic sonography, ^{99m}Tc-DMSA scanning, and RSS within a week of the acute episode. On the basis of laboratory findings, clinical symptoms, and imaging studies, all children received appropriate medical treatment (*3*). For detection and graduation of vesicoureteral reflux, all patients underwent x-ray voiding cystourethrography 1 mo after resolution of the acute episode. All patients entered the follow-up protocol, including both periodic clinical examinations and urine cultures (*3*).

Because an APN lesion takes about 5 mo to stabilize (*9*), ^{99m}Tc-DMSA scanning and RSS were repeated at least 5 mo after UTI was diagnosed (follow-up range, 5–19 mo; mean follow-up, 10 ± 3.5 mo) and after having excluded any other UTI by multiple urine cultures. Renal scarring was diagnosed whenever a cortical defect, detected at the first ^{99m}Tc-DMSA examination, persisted on the follow-up one. Therefore, according to the results of follow-up ^{99m}Tc-DMSA scanning, the examined renal units were retrospectively classified into 2 groups: scarred kidney (SK) and nonscarred kidney (NSK).

^{99m}Tc-DMSA Scanning and RSS Technical Features

^{99m}Tc-DMSA scintigraphy was performed according to our usual clinical protocol. The administered dose was 0.74 MBq/kg of body weight (at least 10 MBq). One posterior projection and 2 posterior oblique projections were recorded beginning 3 h after dose administration, with the patient lying supine and the γ-camera head directly beneath the examination bed. A large-field-of-view γ-camera (ZLC; Siemens) interfaced with an ICON workstation (Siemens) was equipped with a low-energy (140 keV), ultra-high-resolution collimator for a 128 × 128 matrix acquisition. The total count of each image was 500,000. Images were stored on computer to allow digital image enhancement for better evaluation. An experienced observer, unaware of the other patient data, evaluated the images. Renal parenchymal involvement seen on ^{99m}Tc-DMSA scans was graded as 0 (normal), 1 (1 lesion), 2 (2 lesions), or 3 (diffuse damage with renal parenchymal subversion).

RSS was performed using the same modalities and γ-camera as were used for ^{99m}Tc-DMSA scintigraphy. Twenty to 75 MBq of ^{123}I-OIH were prepared in a 5-mL syringe, and the contained volume was increased to 2 mL with saline. Before the patient examination began, the syringe was positioned on a specially prepared 5-cm-thick acrylic support and placed in contact with the collimator surface on the examination table. Activity was measured by the γ-camera; one 50-s static image was acquired in a 64 × 64 matrix by a 20% window centered over the ^{123}I 159-keV energy peak. After this measurement, ^{123}I-OIH was injected as a bolus and data were acquired by a 2-phase dynamic acquisition (80 frames × 5 s per frame and 65 frames × 20 s per frame). After the examination, the depth of the kidney was measured on 1 lateral view by a ^{57}Co-marker.

Cl was then computed by a method and proprietary program previously validated at our institution (*10,11*). This method is based on time–activity curves measured on the heart and kidney areas by the region-of-interest technique. Reference *Cl* values for an age-matched population were previously established to be 333 ± 49 mL/min/1.73 m^2 of body surface area (BSA) (*12*).

X-ray voiding cystourethrography was performed without sedation 1 mo after APN, and the results were reported by an expert pediatric radiologist. All children were previously prepared by preventive treatment with broad-spectrum antibiotics. The bladder was catheterized by a Foley catheter and gently filled with radiographic contrast material. The children then voided during fluoroscopy. According to the recommendations of the International Reflux Study in Children (*13*), a grade of 1–5 was assigned to indicate the severity of vesicoureteral reflux.

Statistical Analysis

All results are expressed as mean ± SD. The relationship between ^{99m}Tc-DMSA scores and the *Cl* variable was assessed by the Spearman nonparametric regression coefficient. ANOVA and Tukey post hoc testing were used for between-group comparisons. Proportions were compared through the Fisher exact test. Univariate discriminant analysis was performed on the variable *Cl* (relative to the inflammatory acute phase) to linearly best discriminate (predictive value) between healthy and scarred renal units on the control ^{99m}Tc-DMSA scans. This procedure computes a linear function yielding the optimal possible classification of observations, taking the result of control ^{99m}Tc-DMSA scanning (NSK or SK) as the grouping factor. The achieved classification, after cross-validation, was submitted to a jackknife validation procedure to limit bias in the number of patients correctly classified. Paired analysis of receiver operating characteristic (ROC) curves was used to compare tests (^{99m}Tc-DMSA and RSS).

The STATISTICA (STATSOFT) and the MiniTab Statistical Software (MINITAB) packages were used for statistical data anal-

TABLE 1
Results of ^{99m}Tc-DMSA Scanning and ^{123}I-OIH Renal Sequential Scintigraphy Performed During Acute Pyelonephritis

No. of renal units	^{99m}Tc-DMSA grade	Unilateral ^{123}I-OIH clearance rate (mL/min/1.73 m^2 BSA)	
		Mean ± SD	Range
40	0	292 ± 33*	237–350
49	1	237 ± 39†	135–300
21	2	210 ± 54†	110–358
6	3	140 ± 53*	47–204

*$P < 0.001$.
†Not statistically significant.

ysis. The software used for paired analysis of ROC curves was Computational Methods for Diagnostic Tests (Freie Universität Berlin). $P < 0.05$ was considered statistically significant.

RESULTS

Staging Evaluation

All children presented with high fever (≥38.5°C), with 9 showing a failure to thrive and 5 having hip pain. All children had a positive urine culture (10^5–10^6 CFU/mL) and an abnormal level of C-reactive protein (0.3–20 mg/L) accompanied by high values for both sedimentation rate (>30) and white blood cell count ($1.4–2.0 \times 10^4$/mm^3). The patients showed no sign of acute renal failure or dehydration on either ^{99m}Tc-DMSA scanning or RSS.

Sonography showed signs suggestive of APN in 40 kidneys (bilateral in 16 children; unilateral in 8 children) and had negative findings in the remaining 76 kidneys.

^{99m}Tc-DMSA scanning showed renal damage in 76 of 116 kidneys (bilateral in 20 children; unilateral in 36 children): 40 renal units were graded 0, 49 were graded 1, and 21 and 6 were graded 2 and 3, respectively (Table 1). The remaining 40 kidneys did not show parenchymal damage (2 patients had bilaterally negative findings). None of the ^{99m}Tc-DMSA findings were equivocal. Table 1 shows the *Cl* values measured for the different classes of renal damage according to the ^{99m}Tc-DMSA results. *Cl* values differed significantly from each other ($P < 0.001$), with the exception of the values for grade 1 versus grade 2 (Fig. 1).

Regression analysis showed a significant relationship between morphologic (^{99m}Tc-DMSA grading) and functional (*Cl* values) renal damage ($R = 0.69$; $P < 0.0001$).

According to the voiding cystourethrography, 40 of 116 examined kidneys had grade I–IV primary reflux. ^{99m}Tc-DMSA scanning had positive findings in 34 kidneys affected by vesicoureteral reflux (85%). Of 76 kidneys without signs of reflux, ^{99m}Tc-DMSA scanning had positive findings in 42 (55%) (Table 2). The incidence of parenchymal ^{99m}Tc-DMSA deficits was significantly different according to the presence or absence of reflux ($P < 0.02$).

Follow-up Evaluation

Follow-up was completed for all patients 5–19 mo (mean, 10 ± 3.5 mo) after staging. All children underwent ^{99m}Tc-DMSA scanning and RSS. Follow-up ^{99m}Tc-DMSA showed persistent renal damage (scarring) in 40 of 76 kidneys and complete recovery in 36 kidneys, of which 28 and 8 were classified as grades 1 and 2, respectively, at staging (recovery rate, 47.4%). In none of the children with normal ^{99m}Tc-DMSA findings at staging did any parenchymal abnormalities develop. Hence, ^{99m}Tc-DMSA findings were classified as follows: 76 as grade 0, 32 as grade 1, and 6 and 2 as grades 2 and 3, respectively (Table 3). Indeed, among 21 kidneys classified as grade 2 at staging, 5 demonstrated an unchanged uptake pattern and 8 showed an improvement in scar grade (grade 1). Among the 6 kidneys classified as

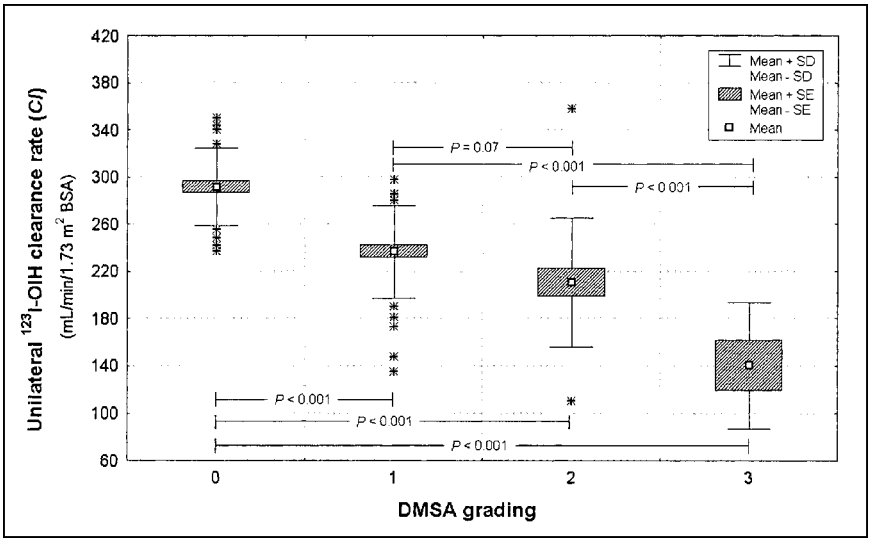

FIGURE 1. Staging ^{123}I-OIH *Cl* in all 116 examined kidneys, classified into 4 groups on basis of uptake pattern of ^{99m}Tc-DMSA scan obtained during APN. * = outliers.

TABLE 2
Results of X-Ray Voiding Cystography Performed 1 Month After APN

VUR	No. of renal units	VUR grade (I–IV)	Staging ^{99m}Tc-DMSA No. of renal units	%	Result
Present	40	I: 15 II: 15 III: 7 IV: 3	34 6	85 15	P N
Absent	76	—	42 34	55 45	P N

VUR = vesicoureteral reflux; P = pathologic DMSA parenchymal uptake; N = normal DMSA parenchymal uptake.

grade 3 at staging, 2 showed persistent unchanged renal scarring and 4 showed an improvement in scintigraphic pattern to grade 2 (1 kidney) or grade 1 (3 kidneys).

Table 3 shows the values of *Cl* measured for the different classes of renal damage according to ^{99m}Tc-DMSA scintigraphy. The reported *Cl* values differed significantly from each other, with the exception of the values for grade 1 versus grade 2 ($P < 0.001$).

Retrospective Analysis

With the presence or absence of parenchymal scarring at follow-up ^{99m}Tc-DMSA scanning considered the grouping factor, all studied kidneys were retrospectively categorized into 1 of 2 groups: NSK or SK.

The 1-way ANOVA applied to all staging parameters (age, temperature at presentation, duration of fever and symptoms, C-reactive protein, sedimentation rate, white blood cell count, CFU, and *Cl*) showed a significant difference only for *Cl* ($P < 0.0001$).

At staging RSS, mean *Cl* values were 260 ± 26 and 187 ± 44 mL/min/1.73 m^2 of BSA for the NSK and SK groups, respectively ($P < 0.0002$). At the following RSS, mean *Cl* values were 291 ± 32 and 246 ± 54 mL/min/1.73 m^2 of BSA for NSK and SK, respectively ($P < 0.0002$). A significant difference between groups ($P < 0.0001$) was found for *Cl* (Table 4; Fig. 2).

^{99m}Tc-DMSA grading was best able to detect acute lesions with a favorable evolution when 2 different ^{99m}Tc-DMSA grades were considered as decisional cutoff values. When grade 1 was selected as the cutoff value, kidneys graded 0 or 1 at staging were considered to have a good prognosis and those graded 2 or 3 were considered to have a bad one. When this criterion was applied, 87 of 116 kidneys were correctly classified, with a specificity, sensitivity, positive predictive value, negative predictive value, and overall accuracy of 89%, 47%, 70%, 76%, and 75%, respectively (Table 5).

Grade 2 was selected as the second cutoff value; in this case, grades 0, 1, and 2 were considered indicators of complete parenchymal recovery and grade 3 was considered an indicator of scar development. When this cutoff was used, 82 of 116 kidneys were correctly classified, with a specificity, sensitivity, positive predictive value, negative predictive value, and overall accuracy of 100%, 15%, 100%, 69%, and 71%, respectively (Table 5).

To differentiate the NSK group from the SK group, the *Cl* cutoff value was determined, for staging *Cl* values, by univariate discriminant analysis: 232 mL/min/1.73 m^2 of BSA discriminated best between the SK and NSK groups. Using this *Cl* cutoff value, the classification matrix was derived. The *Cl* variable correctly predicted the evolution of acute damage in 110 of 116 kidneys, with a specificity, sensitivity, positive predictive value, negative predictive value, and overall accuracy of 95%, 95%, 90%, 97%, and 95%, respectively (Table 5). RSS failed to correctly classify 6 kidneys, having false-negative findings for 4 and false-positive findings for 2.

Matched-pair analysis of the ROC curves showed a significant difference between those derived from the ^{99m}Tc-DMSA and RSS data ($P < 0.0001$).

TABLE 3
Results of Follow-up ^{99m}Tc-DMSA Scanning and ^{123}I-OIH Renal Sequential Scintigraphy

No. of renal units	^{99m}Tc-DMSA grade	Unilateral ^{123}I-OIH clearance rate (mL/min/1.73 m^2 BSA) Mean ± SD	Range
76	0	302 ± 35*	200–467
32	1	259 ± 41†	175–350
6	2	221 ± 31†	170–257
2	3	103 ± 80*	47–160

*$P < 0.001$.
†Not statistically significant.

TABLE 4
Retrospective Analysis of ^{123}I-OIH *Cl* in Renal Units With or Without Detected Parenchymal Scarring at Follow-up DMSA Scanning

Group	^{123}I-OIH *Cl** Staging	Follow-up	*P*	Δ *Cl* % after 10 ± 3.5 mo follow-up
NSK	260 ± 26†	291 ± 32‡	<0.0001	13 ± 14§
SK	189 ± 44†	246 ± 54‡	<0.0001	35 ± 36§

*Mean ± SD mL/min/1.73 m^2 BSA.
†$P < 0.0002$.
‡$P < 0.0002$.
§$P < 0.0005$.
Δ *Cl* % = (follow-up − staging)/staging × 100 ^{123}I-OIH *Cl*.

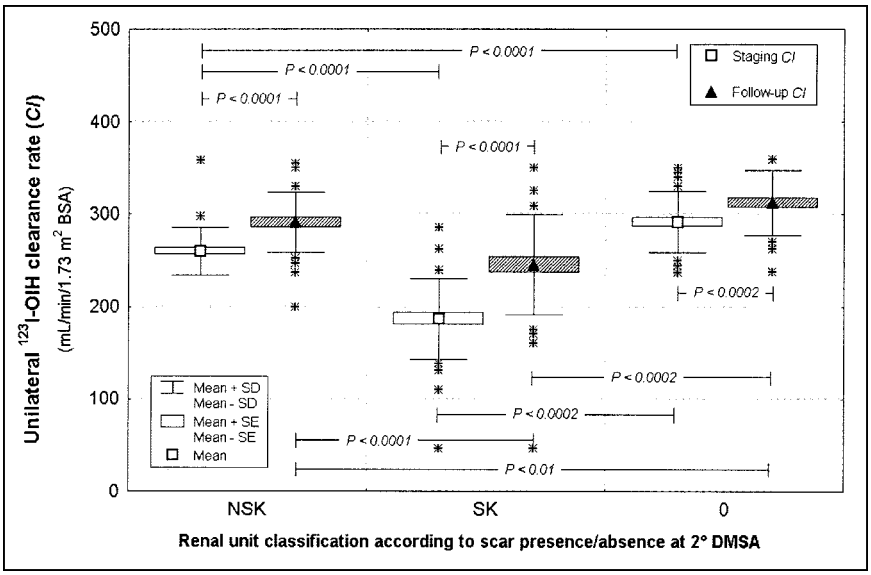

FIGURE 2. Comparison of staging and follow-up ^{123}I-OIH *Cl* in 2 renal subgroups classified on basis of presence or absence of scarring on follow-up ^{99m}Tc-DMSA scan, which was obtained after mean of 10 ± 3.5 mo. Kidneys with normal ^{99m}Tc-DMSA findings at first examination were considered control group. * = outliers.

DISCUSSION

A diagnostic tool that recognizes acute inflammatory processes may be useful in the management of pediatric UTI, especially APN, which has a real risk of resulting in renal parenchymal scarring and, consequently, permanent functional injury of the kidney. ^{99m}Tc-DMSA static planar imaging is largely considered the most sensitive imaging technique for locating and evaluating renal damage in children with APN (*4*,*5*). Besides characterizing the morphology of the parenchyma, ^{99m}Tc-DMSA scintigraphy can also help the clinician evaluate renal functionality using either absolute renal uptake or DRF (*14*,*15*). However, we need a clinically available prognostic parameter that can evaluate the medium- to long-term evolution of ^{99m}Tc-DMSA defects observed during acute infection.

Although DRF has been proposed as a prognostic index, discordant results have been reported. Lavocat et al. (*6*) showed an unfavorable evolution for kidneys that were initially small or had a DRF of less than 45%, but the authors did not mention the global accuracy of the method. Lee et al. (*7*) showed that SPECT DRF was not completely suitable for predicting the permanent sequelae of cortical APN. They reported sensitivity and specificity values similar to those of our study, even if different acquisition modalities were used (SPECT vs. planar). One major limit of DRF arises when an infection involves both kidneys to a varied extent. In such a case, a relative functional estimation is not sufficiently accurate to assess real damage. Durand and Prigent (*16*) proposed an absolute method of ^{99m}Tc-DMSA quantification, but the reported results call for caution in routine clinical use. Recently, Chiou et al. (*17*) suggested morphologic criteria for predicting subsequent renal scarring, that is, analysis of both the region and the intensity of the lesion by acute ^{99m}Tc-DMSA scanning. Using a 4.6-cm^3 cutoff for lesion volume, the authors reported significant results for both sensitivity and specificity in assessing subsequent scar development. Accordingly, in our experience, each kidney classified as grade 3 (diffuse damage with renal parenchymal subversion) at the first ^{99m}Tc-DMSA examination showed permanent parenchymal involvement at follow-up.

TABLE 5
Results of Univariate Discriminant Analysis Performed on ^{99m}Tc-DMSA and *Cl* Data Relative to Inflammatory Acute Phase

Variable	Cutoff	Specificity (%)	Sensitivity (%)	PPV (%)	NPV (%)	Global accuracy (%)
DMSA	Grade 1	89	47	70	76	75
DMSA	Grade 2	100	15	100	69	71
Cl	232	95	95	90	97	95

PPV = positive predictive value; NPV = negative predictive value.

Because tubulointerstitial injury is a primary lesion occurring in the course of APN, an investigation of tubular function would appear to be more useful than the determination of glomerular filtration rate or renal plasma flow. Nevertheless, the role of RSS during APN was demonstrated in both animal and human studies (*18*–*21*). Accordingly, the findings of the present study suggest that *Cl* can be a useful functional absolute parameter during acute UTI to predict the evolution of renal damage detected by ^{99m}Tc-DMSA scanning.

Our results demonstrated a positive correlation between morphologic and functional data (^{99m}Tc-DMSA findings and *Cl*) and confirmed that ^{99m}Tc-DMSA scanning has a good positive predictive value for extended lesions. However, ^{99m}Tc-DMSA scanning also showed a limitation—in predicting the permanent sequelae in cases of few or only a

single APN focus. Indeed, parenchymal focal deficits detected during the first examination were confirmed at follow-up for all 6 renal units classified as ^{99m}Tc-DMSA grade 3 but for only 21 of 49 renal units classified as ^{99m}Tc-DMSA grade 1 (43%). In addition, 96% of ^{99m}Tc-DMSA grade 1 renal units were correctly identified (1 false-positive and 3 false-negative) using the *Cl* cutoff value of 232 mL/min/1.73 m^2 of BSA.

Our results showed that the dimensions of a lesion are not, by themselves, always a valid prognostic factor.

Analysis of renal plasma flow could be a more sensitive method than ^{99m}Tc-DMSA scanning to predict subsequent renal scarring. Even if a functional shock was predictable in the inflammatory acute phase, staging *Cl* values were significantly different between NSK and SK ($P < 0.0002$), likely because of differences in the type of damage and the extent of hypoxia. The same statistically significant difference existed for follow-up *Cl* values, even if the functional recovery is greater for the SK group (Fig. 2; Table 4).

On the whole, our results indicate that both planar ^{99m}Tc-DMSA scanning and ^{123}I-OIH RSS might be useful for grading and characterizing the morphology and function of a single kidney during suspected APN. Such a characterization could be helpful both in diagnosis and in the prognostic stratification of children at real risk of permanent parenchymal injury and, so, worthy of close follow-up (e.g., with biologic indexes and imaging studies).

CONCLUSION

Our data demonstrate that *Cl* assessment during acute UTI is highly valuable in predicting the evolution of renal damage. Moreover, the data also show a close relationship between staging *Cl* and ^{99m}Tc-DMSA grading and confirm the weak relationship between cortical damage and vesicoureteral reflux.

REFERENCES

1. Rushton HG. Urinary tract infections in children: epidemiology, evaluation, and management. *Pediatr Clin North Am.* 1997;44:1133–1169.
2. Hellerstein S. Long-term consequences of urinary tract infections. *Curr Opin Pediatr.* 2000;12:125–128.
3. Subcommittee on Urinary Tract Infection, Committee on Quality Improvement, American Academy of Pediatrics. Practice parameter: the diagnosis, treatment, and evaluation of the initial urinary tract infection in febrile infants and young children. *Pediatrics.* 1999;103:843–852.
4. Jakobsson B, Nolstedt L, Svensson L, et al. ^{99m}Technetium-dimercaptosuccinic acid scan in the diagnosis of acute pyelonephritis in children: relation to clinical and radiological finding. *Pediatr Nephrol.* 1992;6:328–334.
5. Shanon A, Feldman W, McDonald P, et al. Evaluation of renal scars by technetium-labeled dimercaptosuccinic acid scan, intravenous urography, and ultrasonography: a comparative study. *J Pediatr.* 1992;120:399–403.
6. Lavocat MP, Granjon D, Guimpied Y, et al. The importance of ^{99}Tc^{m}-DMSA renal scintigraphy in the follow-up of acute pyelonephritis in children: comparison with urographic data. *Nucl Med Commun.* 1998;19:703–710.
7. Lee BF, Chiou YY, Chuang CM, et al. Evolution of differential renal function after acute pyelonephritis. *Nucl Med Commun.* 2002;23:1005–1008.
8. Groshar D, Embon OM, Frenkel A, et al. Renal function and technetium-99m-dimercaptosuccinic acid uptake in single kidneys: the value of in vivo SPECT quantitation. *J Nucl Med.* 1991;32:766–768.
9. Jakobsson B, Svensson L. Transient pyelonephritic changes on ^{99m}techenetium-dimercaptosuccinic acid scan for at least five months after injection. *Acta Pediatr.* 1997;86:803–807.
10. Formiconi AR, La Cava G, Morotti A, et al. Renal sequential scintigraphy: unilateral clearance rate determination based on external measurements only. *Eur J Nucl Med.* 1983;8:150–154.
11. La Cava G, Sciagrà R, Formiconi AR, et al. Validation of a new method for quantifying renal function. *Contrib Nephrol.* 1990;79:82–86.
12. La Cava G, Sciagrà R, Materassi M, et al. Accuracy of renal sequential scintigraphy for the recognition of renal involvement in paediatric patients affected by urinary tract infection. In: Schmidt HAE, van Schoot JB, eds. *Nuclear Medicine: the State of the Art of Nuclear Medicine in Europe.* New York, NY: Schattauer; 1991:356–359.
13. Lebowitz RL, Olbing H, Parkkulainen KV, Smellie JM, Tamminen-Möbius TE. International system of radiographic grading of vesicoureteral reflux. International Reflux Study in Children. *Pediatr Radiol.* 1985;15:105–109.
14. Goodgold HM, Fletcher JW, Steinhardt GF. Quantitative technetium-99m dimercaptosuccinic acid renal scanning in children. *Urology.* 1996;47:405–408.
15. Groshar D, Gorenberg V, Weissman I, et al. Detection of permanent damage in kidneys with vesicoureteral reflux by quantitative single photon emission computerized tomography (SPECT) uptake of ^{99m}technetium labeled dimercaptosuccinic acid. *J Urol.* 1996;155:664–667.
16. Durand E, Prigent A. Can dimercaptosuccinic acid renal scintigraphy be used to assess global renal function? *Eur J Nucl Med.* 2000;27:727–730.
17. Chiou YY, Wang ST, Tang MJ, et al. Renal fibrosis: prediction from acute pyelonephritis focus volume measured at ^{99m}Tc dimercaptosuccinic acid SPECT. *Radiology.* 2001;221:366–370.
18. Roberts JA, Domingue GJ. Experimental pyelonephritis in the monkey. II. The prognostic value of radionuclide evaluation of the urinary tract. *Invest Urol.* 1975;12:374–380.
19. Fischman NH, Roberts JA. Clinical studies in acute pyelonephritis: is there a place for renal quantitative camera study? *J Urol.* 1982;128:452–455.
20. Janson KL, Roberts JA, Levine SR, et al. Noninvasive localization of urinary tract infection: clinical investigation and experience. *J Urol.* 1983;130:488–492.
21. Sfakianakis GN, Cavagnaro F, Zilleruelo G, et al. Diuretic MAG3 scintigraphy (F_0) in acute pyelonephritis: regional parenchymal dysfunction and comparison with DMSA. *J Nucl Med.* 2000;41:1955–1963.